Probing the Structural Changes in the Light Chain of Human Coagulation Factor VIIa Due to Tissue Factor Association

Lalith Perera,* Thomas A. Darden,# and Lee G. Pedersen*#

*Department of Chemistry, University of North Carolina, Chapel Hill, North Carolina 27599-3290, and #National Institute of Environment Health Science, Research Triangle Park, North Carolina 27709-2233 USA

ABSTRACT   The crystallographic structure of human coagulation factor VIIa/tissue factor complex bound with calcium ions was used to model the solution structure of the light chain of factor VIIa (residues 1–142) in the absence of tissue factor. The Amber force field in conjunction with the particle mesh Ewald summation method to accommodate long-range electrostatic interactions was used in the trajectory calculations. The estimated TF-free solution structure was then compared with the crystal structure of factor VIIa/tissue factor complex to estimate the restructuring of factor VIIa due to tissue factor binding. The solution structure of the light chain of factor VIIa in the absence of tissue factor is predicted to be an extended domain structure similar to that of the tissue factor-bound crystal. Removal of the EGF1-bound calcium ion is shown by simulation to lead to minor structural changes within the EGF1 domain, but also leads to substantial relative reorientation of the Gla and EGF1 domains.

INTRODUCTION

The zymogen factor VII has no activity in its native form in the circulating blood. Activation occurs upon contact with tissue factor (TF), exposed by vascular injury. Once formed, this complex rapidly initiates blood coagulation by proteolytically activating its substrates, factor IX and X, leading to thrombin formation and a fibrin clot. Although earlier studies (Zur and Nemerson, 1978; Jesty and Morrison, 1983) reported that the single chain factor VII demonstrates considerable activity toward substrates, recent experimental data (Wildgoose et al., 1990; Lawson et al., 1992; Chaing et al., 1994) found almost no amidolytic activity. Hence the activation of factor VII (Hagen et al., 1986), a single-chain protein of 406 residues converted to factor VIIa by cleavage of a single peptide bond between Arg^{152} and Ile^{153}, can now be recognized as the primary event that initiates the coagulation cascade by cleavage of factors X and IX (Nemerson, 1988; Lawson and Mann, 1991; Krishnaswamy, 1992; Butenas and Mann, 1996; Tuddenham, 1996; Kirchhofer and Nemerson, 1996). The full enzymatic potential of factor VIIa requires complexation with TF in the presence of calcium ions (Nemerson, 1988; Davie, 1995; Rapaport and Rao, 1995).

Factor VII circulates at very low concentration (10 nM) and has a short half-life of 2–3 h, whether it is in the zymogen form or in its activated form, a property unique among the other vitamin K-dependent coagulation proteases (Petersen et al., 1995). The elevated level of factor VII leads to increased risk of coronary thrombosis (Meade, 1983), and the deficiency of factor VII is associated with either variable bleeding (Triplett et al., 1985) or thrombotic manifestations

(Tuddenham and Cooper, 1994). Serine proteases (SP) including factors IXa, Xa, XIIa, and thrombin have been reported to activate factor VII in vitro, but precisely which of these is responsible in vivo remains unknown. It has been reported (Nemerson and Esnouf, 1973; Sakai et al., 1989; Nakagaki et al., 1992; Yamamoto et al., 1992; Ruf, 1994; Edgington et al., 1997) that the factor VIIa/TF complex may also activate factor VII autocatalytically under physiological conditions. Tissue factor pathway inhibitor (TFPI) can inhibit TF-bound factor VIIa in the presence of factor Xa (Petersen et al., 1995).

The x-ray crystal structure of the factor VIIa/TF complex is available (Kirchhofer et al., 1995; Banner et al., 1995, 1996; Banner, 1997). These coordinates were used to create a model for the factor VIIa light chain in solution. The amino acid sequence of the light chain that contains the Gla domain and two EGF domains is given in Fig. 1, along with the domain definitions. Molecular dynamics simulations, successfully applied in previous studies of other coagulation proteins (Hamaguchi et al., 1992, Li et al., 1995, 1996, 1997; Perera et al., 1997, 1998), can yield atomic-level information about the solution structure of factor VIIa in its TF-free form. (Hereafter, we refer to it as TF-free solution.) Moreover, this TF-free solution structure will serve as a valuable template for predicting the structural changes associated with the formation of the factor VIIa/TF complex and organizing mutational data. Our main focus in the present work is on the structural changes in the Gla and EGF1 domains due to calcium binding and TF association in the EGF1 domain. We will discuss the lipid binding properties of the Gla domain by examining the properties of the calcium-Gla network, the Ω-loop structure, and the spatial arrangements of other potential lipid-binding residues. The function of the calcium ion bound to the EGF1 domain is studied by removing it and comparing the resulting structure, determined by simulation, with the predicted solution structure in the presence of this calcium. Although

FIGURE 1 The amino acid sequence of the segment of the factor VIIa light chain used in the present study. The domain definitions are as follows: Gla domain, residues 1–35; connecting region between the Gla and EGF domains, residues 36–45; EGF1 domain, residues 46–82; connecting residues between the EGF1 and EGF2 domains, residues 83–85; EGF2 domain, residues 86–131; connecting region between the EGF2 domain and the SP domain, residues 132–142. The disulfide loops are also marked. However, in the text, the residues in the Gla-EGF1 connecting region are considered to be part of the Gla domain.
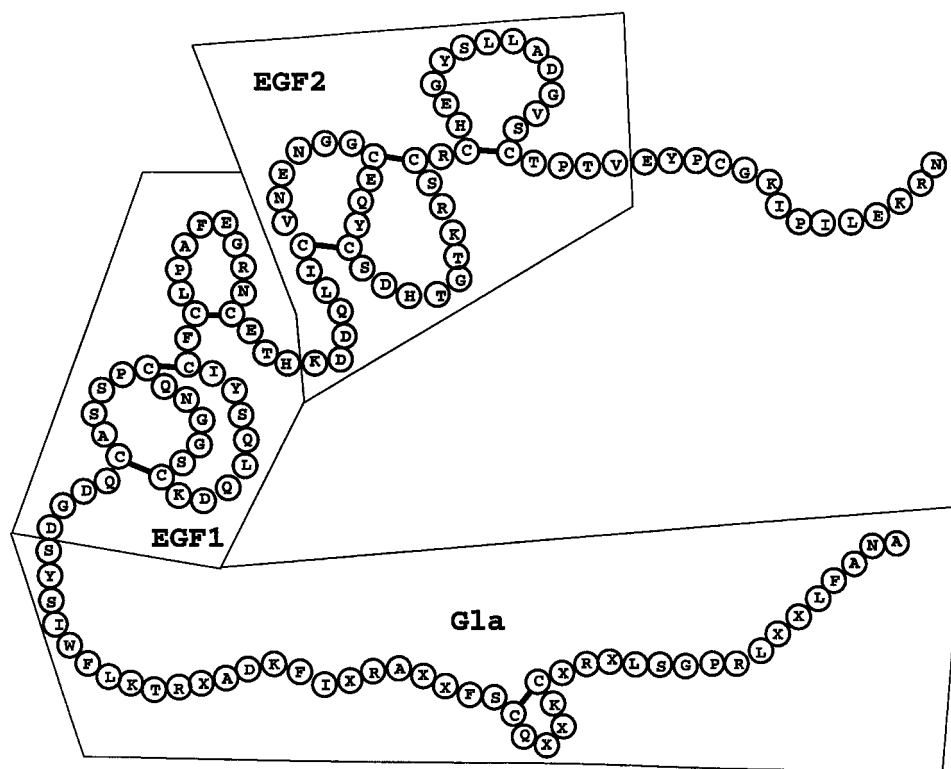
our primary focus is on the Gla-EGF1 fragment of factor VIIa, inclusion of the EGF2 domain is, however, essential for providing a realistic environment for the EGF1 domain.

COMPUTATIONAL PROCEDURE

Model construction and simulation protocol

The initial structures of the model protein (residues 1–142) were derived from the crystallographic coordinates of the factor VIIa/TF/Ca^{2+} fragment (pdb entry = 1dan). Crystallographic water molecules within 5 Å of any protein atom were included, and all of the calcium coordinates assigned in the crystal configuration were preserved in the initial structure. Necessary hydrogen atoms were added to the x-ray crystallographic structure, followed by energy minimization of the side chains, using a distance-dependent dielectric function (500 steepest descent steps followed by 10,000 conjugate gradient steps).

The protein (along with the crystallographic water molecules and the calcium ions) was then solvated in a box of water molecules so that the box boundaries are at least 12.5 Å away from any protein atom. Water molecules used in the solvation of the protein for which the oxygen or hydrogen atoms were found to be within 2.0 Å of any atom in the protein were excluded. The central simulation box contained 142 residues of the light chain of factor VIIa, 16,485 water molecules, and 10 calcium ions. In addition to the eight calcium ions found near the Gla and EGF1 domains of the x-ray crystal structure of TF-bound factor VIIa, two calcium ions were introduced as free nonbound counterions. The two calcium counterions did not coordinate with any of the protein residues at any time during the simulation. The simulation system was thus electrically neutral. The total number of atoms in this box was 51,939. In the first step, only the added water molecules were energy minimized at constant volume (10,000 conjugate gradient steps), then all of the water molecules were subjected to energy minimization (another 10,000 conjugate gradient steps), and finally, the whole system was energy minimized (10,000 conjugate gradient steps). The system was subsequently subjected to a slow heat-up procedure to

bring the temperature of the system to 300 K. After 25 ps of a constant volume/constant temperature simulation, the system was reminimized (20,000 conjugate gradient steps). After another heat-up run of 10 ps to bring the temperature back to 300 K, a constant temperature/constant volume MD run was performed for 25 ps. Finally, a constant pressure/constant temperature protocol was adopted to simulate 600 ps of dynamics.

In the present study, we used the second generation of AMBER force field (Cornell et al., 1995) in conjunction with the particle mesh Ewald method (Essmann et al., 1995) to accommodate long-range interaction in all of the solution simulations. The trajectory calculations were done with AMBER version 4.1 (Pearlman et al., 1995). The time step was 1 fs, with the nonbonded interactions updated at every step in all simulations. This choice of updating nonbonded interactions and the periodical removal of the translational and rotational motions of the center of mass (every 2.5 ps) help prevent artifacts, such as the observation of a "flying ice cube" (Harvey et al., 1998).

The role of the calcium ion bound to EGF1 domain was studied by removing it from the predicted TF-free solution structure of the light chain of factor VIIa. A simulation led to comparison of the TF-free solution structures with and without this ion. The removal of the calcium ion from the EGF1 domain was achieved as follows. As this ion was removed from the vicinity of the EGF1 domain, another calcium ion was created at an appropriate distance from the peptide to maintain the consistency in the constituents of the simulation box. First, a particle having Lennard-Jones parameters (ϵ and σ) similar to the ones used for calcium ions in the present study was created at a location at least 15 Å from any protein atom. This particle was grown while fixing ϵ at ϵ_{Ca} and incrementally changing σ, from 10% of σ_{Ca} initially, to full value. The creation of the new particle was completed during a 30-ps dynamical trajectory. During the next 100 ps of the trajectory, the charge of the calcium ion bound to EGF1 was reduced stepwise from its full value ($+2e$) to zero while an equivalent amount of charge was added to the new particle. This process converts the new particle to a calcium ion and the calcium ion initially bound to the EGF1 domain to an uncharged particle. The subsequent stepwise reduction of ϵ from its original value to zero over 100 ps removes this particle from the simulation box. This procedure removes the calcium ion bound to EGF1

domain and places its solvated successor in another part of the central simulation box with no direct interactions with any of the protein atoms. Finally, a shake-up procedure to improve dynamical sampling was implemented to accelerate the events (if any) following the removal of the calcium bound to the EGF1 domain. In this procedure, the system was heated up to 350° K over 25 ps of dynamics, and the temperature was maintained at 350° K for an additional 25 ps. The temperature was reduced to 300° K during the next 25 ps of dynamics and was maintained at 300° K for the remainder of the trajectory calculation (a total of 1.445 ns).

RESULTS AND DISCUSSION

Global aspects of the simulation

Molecular dynamics simulation methods have proved to be a valuable complementary tool for obtaining molecular-level information of the protein structures in solution. However, one must take considerable precautions in predicting solution structures from dynamical simulations to ensure that the systems in consideration reach equilibrium. Inadequate simulation times and inappropriate methodology for determination of long-range interactions can lead to difficulties. Thus it is essential to provide testing to achieve stability. Currently, in addition to the realization of constancy in the potential energy as a measure of the stability of the system, simulators use RMSDs with respect to the crystal configuration or to the initial minimized configuration (Hamaguchi et al., 1992; Li et al., 1995; Perera et al., 1997). Another, more useful calculation for multidomain proteins is to evaluate the individual RMSDs for each domain (for example, Gla, EGF1, and EGF2 in the present case). This procedure can yield information on how particular domains restructure because of the presence of solution, absence of crystal contacts, or inclusion/absence of ions. The RMSDs calculated from the union of domains are essential for obtaining details of interdomain motion. In Fig. 2, we display the RMSDs of the entire peptide (residues 1–142), the Gla domain (residues 1–35), the EGF1 domain (residues 46–84), the EGF2 domain (residues 85–131), and the Gla/EGF1 (residues 1–84) and EGF1/EGF (residues 45–131) unions. We focus on the results of RMSD up to 600 ps because at this time the removal of the calcium ion bound to the EGF1 domain is initiated (discussed in a later section). Smaller fluctuations in all of the values of RMSDs during the 400–600-ps segment of the simulation ensure the stability of the system in solution. The displacements of the backbone atoms of the individual Gla and EGF1 domains with respect to their x-ray crystal positions remain relatively small (the final values of the RMSD fluctuate around 0.5 Å for these two domains). The deviation of the EGF2 domain with respect to the x-ray crystal structure shows a relatively larger magnitude (around 1.8 Å) compared to the Gla and EGF1 domains. This is to be expected, because the EGF2 domain loses a number of contacts with the SP domain, and the latter is excluded from the present model calculation. On the other hand, the combined Gla/EGF1 and EGF1/EGF2 domains show somewhat larger magnitudes in their RMSD values than the individual domains. As has been pointed out
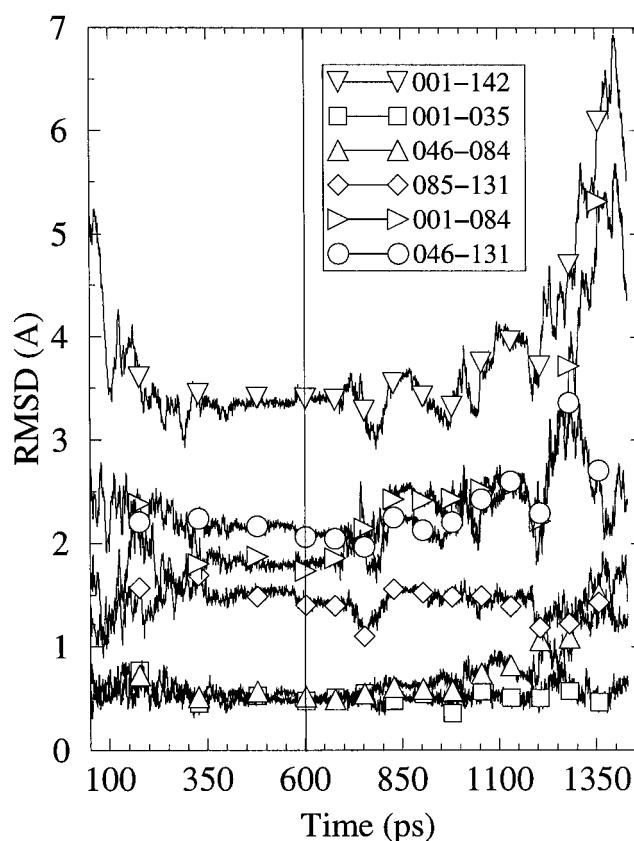

FIGURE 2 Root mean square deviations (RMSDs) of the backbone atoms, calculated with respect to the positions of atoms in the x-ray crystal configuration of the factor VIIa/TF complex. In addition to residues 1–142, which comprise all three domains (Gla, EGF1 and EGF2), the RMSDs of individual Gla, EGF1, and EGF2 domains are included. The RMSDs calculated for combined domains, Gla/EGF1 and EGF1/EGF2, are displayed to probe possible interdomain separations.

earlier (Hamaguchi et al., 1992), such deviations may arise because of relative domain motions, even though individual domains remain relatively near the TF-bound crystal structure. When the combined three-domain structure is considered, the net reorganization effect is amplified in the RMSD curve (RMSD = 3.5 Å). The density fluctuations of the system, found to be small ($\rho = 1.04 \pm 0.02$ g/cc) during the final 100-ps interval, provide additional support for system stabilization.

The simulation B-factors, calculated for backbone atoms by averaging over the 350–600-ps segment of the trajectory, are given in Fig. 3. The general trends show that the backbone atoms in the TF-free solution structure are relatively stabilized around their average positions, and the fluctuations around the average positions are on the order of an angstrom. The residues that exhibit significantly larger movements through their B-factors compared to the majority of the residues, with the exception of His[84], are glycine residues (58, 59, and 107). None of these residues, including His[84], have H-bonds with the other residues. Likewise, none were found to have crystal contacts with any other residue in factor VIIa (both light and heavy chains taken together)
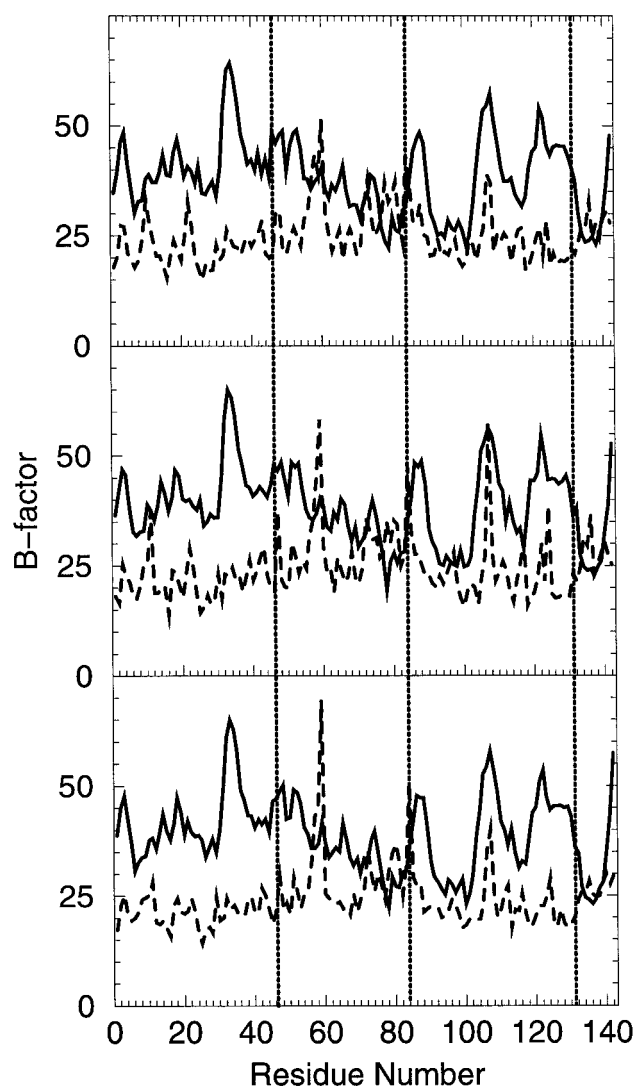
FIGURE 3   Experimental (for x-ray crystal factor VIIa/TF: ——) and calculated (for factor VIIa solution: – – –) B-factors of backbone atoms (N (*top*), C_α (*middle*), and carbonyl C (*bottom*)) of the residues (1–142). The domain boundaries are indicated by vertical lines.

or with TF (when factor VIIa is bound in the crystal configuration).

The final predicted TF-free solution structure was checked using the program PROCHECK (Laskowski et al., 1993) to evaluate the "goodness" of the geometrical entities such as bonds, angles, and dihedral angles in the average molecular structure of the solution protein when compared with those found in the crystal. The PROCHECK comparison showed no major discrepancies. Although Lys[32] of the x-ray crystal structure of TF-bound factor VIIa falls in the disallowed region according to the values for its Phi/Psi angles, the angles associated with this residue in the TF-free solution structure are found within the acceptable values.

Gla domain

The Gla domain and the following hydrophobic stack have been shown to be important for the optimal interaction

between factor VIIa and TF (Persson, 1996). Likewise, it has been suggested that this fragment is important for macromolecular substrate recognition (Martin et al., 1993). The Gla domain of factor VII contains 10 Gla residues. Of the nine calcium ions found in the x-ray crystal structure of TF-bound factor VIIa, seven are present near the Gla region. These calcium ions participate in the formation of the Gla-calcium network. The effect of the calcium ions on the structure and function of factor VIIa and the affinities of the calcium binding have been subjected to extensive studies by several laboratories (Cheung and Stafford, 1995; Persson and Petersen, 1995; Persson, 1996, 1997; Petersen and Persson, 1996; Freskgard et al., 1998; Inoue et al., 1996). Geng and Castellino (1997) studied the lipid-binding properties of a recombinant chimeric protein in which the Gla and helical stack domains of human anticoagulant protein C were replaced by those of human factor VII. They observed that the chimeric protein maintains the calcium/phospholipid-related functions of protein C and suggested, on the basis of similarity to factor VIIa, that the general calcium ion-dependent membrane-binding properties are very similar in the vitamin K-dependent coagulation proteins. However, the actual degree of affinity of lipid binding may depend on the sequence specificity found in different VKD proteins. For example, protein C and factor VII do not contain a Gla residue at position 33, and they both have low affinity toward membranes (McDonald et al., 1997a,b).

We compare the Gla domain (residues 1–45) solution structure with that of the factor VIIa/TF in crystal (Fig. 4). The displacements, on average, are found to be relatively small, even for the side chains (the RMSD for the backbone and all heavy atoms in this domain is 1.40 Å). However, some change in the backbone dihedral angles associated with Gla[7] and Gla[35] occur during the dynamics. The computed B-factors in the TF-free solution simulation for Gla[35] (Fig. 3) are normal, whereas they are elevated in the x-ray crystal structure of TF-bound factor VIIa. Even though Gla[35] does not participate in the Gla-calcium network, the backbone carbonyl oxygen makes a strong intramolecular H-bond with the backbone N of Leu[39] in the crystal. Whereas this interaction remains stable in the TF-free solution structure, an additional intramolecular H-bond was found between the side chains of Gla[35] and Lys[38] in solution. Persson and Nielsen (1996) found that if Gla[35] is mutated to Asp, Gln, or Val, the resulting variant has a lower affinity for TF measured by surface plasmon resonance. However, the mutation Gla[35]-Glu did not affect TF binding (Persson and Nielsen, 1996). A closer look at the TF-bound structure reveals that Gla[35] is situated at a distance sufficient to form a salt bridge with Lys[165] in TF. Gla[35] is found to be solvent exposed in both the x-ray crystal structure of TF-bound factor VIIa (156 Å^2) and the TF-free solution structure (147 Å^2). These values are larger than the solvent-accessible area of other Gla residues, and hence one can reasonably assume that there is potential for a salt bridge of Gla[35] in factor VIIa with TF that enhances the association of factor VIIa/TF complex.
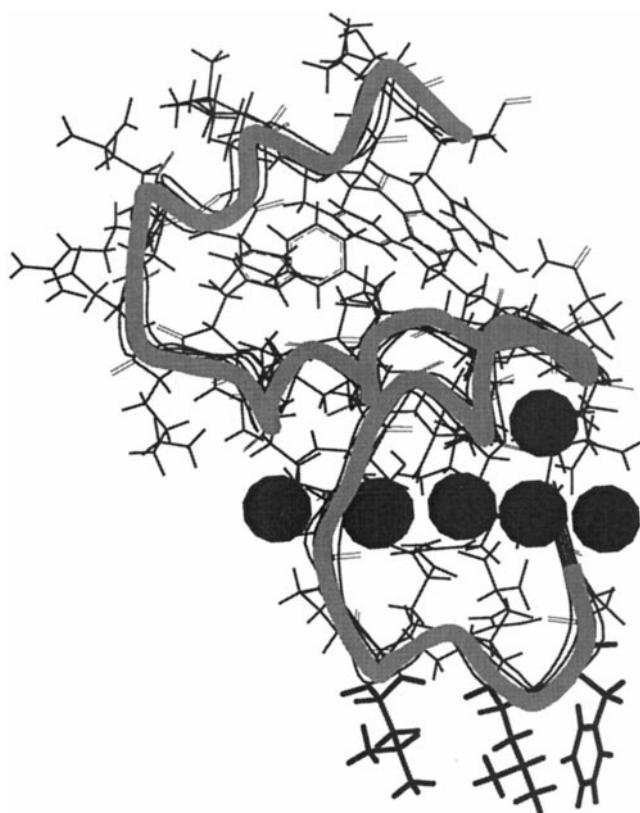
FIGURE 4 Comparison of the final TF-free solution structure (600 ps) of the Gla domain of factor VIIa residues 1–45 with that of the factor VIIa/TF crystal complex. The backbone ribbons are used to represent the secondary structure (solution: *light band*; crystal: *line ribbons*). The two structures were aligned using the best fit of the backbone atom positions. Changes in the secondary structure are essentially indistinguishable. Amino acid residues are represented, only for the solution structure, by lines, and calcium ions are represented by dark circles. The Ω-loop, which is thought to participate in lipid interaction, is clearly visible at the base of the structure.

Several of the calcium ions moved somewhat closer to Gla residues, forming stronger ionic bonds with them once introduced to the solution (for example, Ca-3 and Ca-9). However, no major restructuring in the Gla-calcium network (Table 1) is observed to be due to solvation. Most of the crystallographic water molecules remained coordinated to calcium ions during our simulations, emphasizing the stability of those water molecules in the structure determination. The N-terminus Ala[1] network is also preserved during the TF-free solution simulation (Table 2). In bovine prothrobin fragment I (BF1), this network was recognized to be responsible for the formation of the Ω-loop that undergoes the required folding for lipid binding in the presence of calcium ions (Welsch and Nelsestuen, 1988). Taken together, the stability in the Gla-calcium network and the conservation of both the Ala[1] network and Ω-loop in solution indicate that lipid-binding properties similar to BF1 can be expected for the factor VII/Ca complex, even in the absence of TF.

Residues Lys[18], Arg[36], and Ser[43] in the Gla domain are found to be in the close vicinity of TF in the crystal configuration (<3.2 Å) and in fact, several of the side-chain atoms of these residues are close enough to make strong H-bonds with side chains of the residues in TF. For example, NH1 of Arg[36] is within 2.7 Å of OG of Ser[163] in TF. This interaction site is in close vicinity to the possible Gla[35] (in factor VII) and Lys[165] (in TF) interaction site discussed above. In the TF-free solution structure, both Gla[35] and Arg[36] are found to have large solvent accessibilities, indicating their availability for possible H-bonds when TF comes in contact with factor VII. However, Lys[18] is intradomain H-bonded to Leu[13] in both TF-bound crystal and TF-free solution configurations. On the other hand, Arg[36] has an intradomain H-bond to Asp[33] only in the crystal configuration, whereas Ser[43] does not possess intradomain H-bonds in either structure. The observed intradomain H-bonds of Lys[18] in the TF-free solution structure may compete with the propensity of this residue to form H-bonds with TF residues. It is interesting to note that no mutation with severe clinical manifestations has been found so far in the factor VIIa Gla domain, although there is an interesting heterozygous mutation (Gla[16]-Lys) (Tuddenham and Cooper, 1994; Tuddenham et al., 1995; Cooper et al., 1997).

EGF1 domain

Several residues of the EGF1 domain found to directly interact with TF have been shown to be substantially responsible for factor VIIa/TF affinity, using mutational analysis of factor VIIa (Kelly et al., 1997). Because the present simulation is performed in the absence of TF, comparison of the TF-free solution structure to that of TF-bound crystal may help one understand the consequences of the removal of TF. In other words, observed structural changes (if any) in factor VIIa may be partially attributed to the association with TF. The RMSD values corresponding to the EGF1 domain indicate that the backbone atoms do not undergo appreciable structural changes when solvated (and separated from) the TF-bound crystal. For comparison, we display (Fig. 5) the TF-free solution structure of EGF1 domain and the superimposed backbone structure of the same domain in the TF-bound crystal. As can be seen from the figure, the backbones align quite well, indicating that the changes in the secondary structure are minimal. It thus appears that the TF association does not cause significant secondary structural changes in the EGF1 domain.

Factor VII contains two Gla-independent calcium-binding sites (as do factors IX and X and protein C). One of these sites is found in the EGF1 domain of factor VII. Protein C and factor X contain an aspartic acid residue in the first EGF domain that is postribosomally hydroxylated to erythro-β-hydroxyaspartic acid. The analogous residue is partially hydroxylated in factor IX. A consensus sequence that appears to be required for the modification has been proposed (Thim et al., 1988). Even though factor VII has the consensus sequence in its EGF1 domain, neither plasma-derived or recombinant factor VII has been shown to con-

TABLE 1 Ca^{2+}-Gla interactions ($d_{Ca-Gla} \leq 3.0$Å) for the crystal structure of factor VIIa/TF complex (top line) versus the TF-free solution structure of factor VIIa (bottom line)

	Gla									Water	Other	Total
Gla→	06	07	14	16	19	20	25	26	29			
	1234	1234	1234	1234	1234	1234	1234	1234	1234			
		0101						0100	0011	2 (2)		7
Ca-3		0101					1000	0100	0011	1		7
		1100		0010				1000	0001	3 (3)		8
Ca-4		1100		0010				1000	0001	3 (3)		8
	1000	1000		1010				1001		NO	1	7
Ca-5	1100	1000		1010				1001		NO	1	8
	1001			1100		0011				1 (1)	1	8
Ca-6	1001			1100		0011				1	1	8
			0110		0110					1 (1)		5
Ca-7			0110		0110					3		7
						1010				NO		2
Ca-8						1010				6		8
							1000		1010	NO		4
Ca-9							1010		1010	4		8

The results were averaged over the last 20 ps of the trajectory for the solution structure (600 ps). The number of water molecules given in parentheses represents the crystal water. (NO = no water molecules found in the crystal configuration.)

tain erythro-β-hydroxyaspartic acid at position 63 (Thim et al., 1988). This modification, however, does not appear to affect calcium binding (Selander-Sunnerhagen et al., 1992; Sunnerhagen et al., 1993, 1995) in EGF1 of factors IX and X. Because calcium binding involves mostly the residues in the Gla-EGF1 connecting region, we will defer a discussion on details of the calcium binding to a subsequent section.

It has been found that the naturally occurring mutation Asn[57]Asp in the EGF1 domain (Berube et al., 1992) affects the folding of this domain and subsequently decreased cellular secretion of mutant factor VII. The mutant protein does not bind TF and is therefore present in an apparently biologically inactive form (Leonard et al., 1998). Furthermore, the natural mutation Arg[79]-Gln in the EGF1 domain may reduce the affinity for TF binding (O'Brien et al., 1994; Takamiya et al., 1995). The side chains for all EGF1 residues in the TF-free solution structure are displayed in Fig. 5. Residues Asp[57] and Arg[79] are represented by thicker sticks in Fig. 5. The residues Lys[62], Gln[64], Ile[69], Phe[71], and Arg[79] show significant impact on TF binding in the alanine scanning mutagenesis experiments on factor VII (Dickinson

TABLE 2 Comparison of the Ala[1]-N network of the solution structure of factor VIIa in its TF-unbound form with the factor VIIa/TF in the crystal

Crystal	Ala[1]-N	Gla[20]-OE4	2.5	163
	Ala[1]-N	Gln[21]-O	3.0	156
	Ala[1]-N	Gla[26]-OE4	2.8	155
	Ala[1]-N	Ca-4	4.34	
	Ala[1]-N	Ca-5	3.85	
Solution	Ala[1]-N	Gla[20]-OE4	2.8	173
	Ala[1]-N	Gla[16]-O	2.7	152
	Ala[1]-N	Gla[26]-OE4	2.9	159
	Ala[1]-N	Ca-4	4.42	
	Ala[1]-N	Ca-5	4.07	

The distances and angles were averaged over the last 20 ps of the simulation. The cutoff distance and angles were 3.0 Å and 115°, respectively.

et al., 1996; Dickinson and Ruf, 1997). Analysis of the TF-bound crystal structure shows that residues Lys[62], Gln[64], Leu[65], Ile[69], Cys[70], Phe[71], Cys[72], Leu[73], Pro[74], Glu[77], Gly[78], and Arg[79] are either in close contact with or in the near vicinity (within 4 Å) of TF residues (Banner et al., 1996). These residues are somewhat confined to a planar surface (base of Fig. 5), which prevents Asn[57] from directly participating in TF binding in the solution structure. This residue is positioned in a critical turn and thus may be essential for proper folding of the EGF1 domain (Leonard et al., 1998). It is also noteworthy that Asn[57] is conserved in most EGF1 domains except protein S and protein C. In fact, the strong intradomain H-bond found between Asn[57] and Cys[81] in the TF-bound crystal structure of factor VIIa is preserved during the entire solution simulation. On the other hand, Arg[79] is found to be directly involved in TF binding in the x-ray crystal configuration. This residue is highly solvent accessible (solvent-accessible area 212 Å²) in the TF-free solution structure and makes no intramolecular H-bonds with any other residue. As ecxpected, almost all of the residues that participate in the TF binding in the TF-bound crystal configuration are found to be highly solvent accessible in the TF-free solution structure.

It is of interest whether significant side-chain movements in the interface of the EGF1 domain with TF (described above) occur because of TF binding to this interface. We can analyze the side-chain movement of the interface of the EGF1 domain with TF by comparing the B-factors calculated for the heavy atoms of the side chains with the corresponding B-factors from x-ray experiment. The B-factors of the side chains in the TF-free solution, in general, are somewhat smaller than the TF-bound crystal form, and this follows a similar observation for backbone atom B-factors given in Fig. 3. As evident from Fig. 6, some of the residues (Lys[62], Gln[64], Leu[65], Phe[71], Leu[73], and Arg[79]) that were in close contact with or in the vicinity of TF show larger
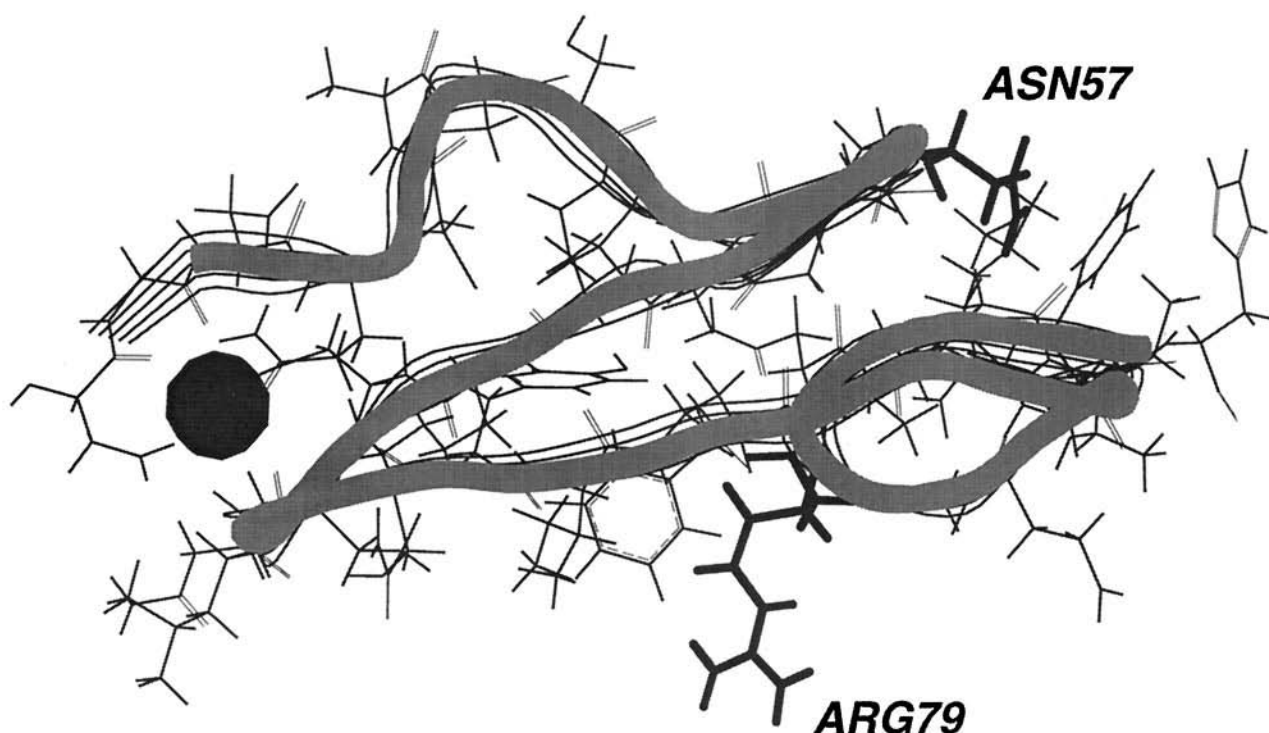
FIGURE 5 Comparison of the final TF-free solution structure (600 ps: *light band*) of the EGF1 domain of factor VIIa with that of the factor VIIa/TF x-ray crystal complex (*line ribbons*). The least-squares fit of the backbone atoms was used for the alignment. Side chains are displayed for the solution structure. The two residues (Asn[57] and Arg[79]), which are involved in TF binding, are especially marked. All of the residues that participate in TF binding are seen at the base of the figure (along with Arg[79]).

B-factors in TF-free solution and, certainly, some of these B-factors are larger than the experimentally reported values in the TF-bound crystal. Except in the case of Lys[62] and Arg[79], which are ionic side chains, the other residues may not be extended very much into water because of the hydrophobic nature of these residues. Because in binding with TF these residues were somewhat extended, in solution they find it more appropriate to cluster with the other hydrophobic residues in the aqueous environment.

Carbohydrate chains attached to the *O*-glycosylation sites (Ser[52] and Ser[60]) in the EGF1 domain of factor VII in the TF crystal complex were not included in our present TF-free solution structure calculation. Two serine residues in the EGF1 domain of factor VIIa, Ser[52] and Ser[60], are reported to support carbohydrate linkages (Bjoern et al., 1991). A trisaccharide, or a truncated form of a longer carbohydrate, is *O*-glycosidically linked to Ser[52] of human factor VIIa (Bjoern et al., 1991). There are similar reports of carbohydrate attachment at this position for bovine factors VII and IX, human factor IX, and human and bovine protein Z (Nishimura et al., 1989). Ser[60] contains an *O*-glycosidically linked fucose fragment (Bjoern et al., 1991; Harris et al., 1991). The direct biological function of the carbohydrate attachment is as yet unknown, but mutations at Ser[52] and Ser[60] (by Ala) show reduced clotting activity in factor VII (Iino et al., 1998). Iino et al. (1998) also found indistinguishable changes in TF-dependent and TF-independent amidolytic activity for mutants compared to the wild type.

The possible glycosylation site of the nearby Ser[53] residue, in both TF-bound crystal and TF-free solution, is directed somewhat toward the interior of the protein and hence is less accessible for glycosylation. Furthermore, in both TF-free solution and TF-bound crystal, we find that the side chain of Ser[53] forms two intramolecular H-bonds as opposed to a single intramolecular H-bond found in each Ser[52] and Ser[60], thus reducing the possibility of forming the carbohydrate link.

EGF2 domain

The focus of the current work is on the Gla-EGF1 domains. The EGF2 domain, however, was included in the present calculation to provide a more realistic environment, especially for the EGF1 domain. Changes that we find in the TF-free solution structure of EGF2 domain must be due to loss of TF contacts, but also to lack of EGF2-SP domain contacts. Thus caution is warranted in interpreting the EGF2 simulation structure. That aside, we find that whereas the EGF2 RMSD is somewhat larger (Fig. 2) than the individual Gla and EGF1 domain RMSDs, the long axis of the peptide Gla-EGF1-EGF2 does not change appreciably during the simulation. Similarly, the overall fold of EGF2 is maintained (Fig. 7), although some change occurs in the connecting segments between EGF1 and EGF2 (residues 85–93) and in the segment 103–111. Only a few of residues of
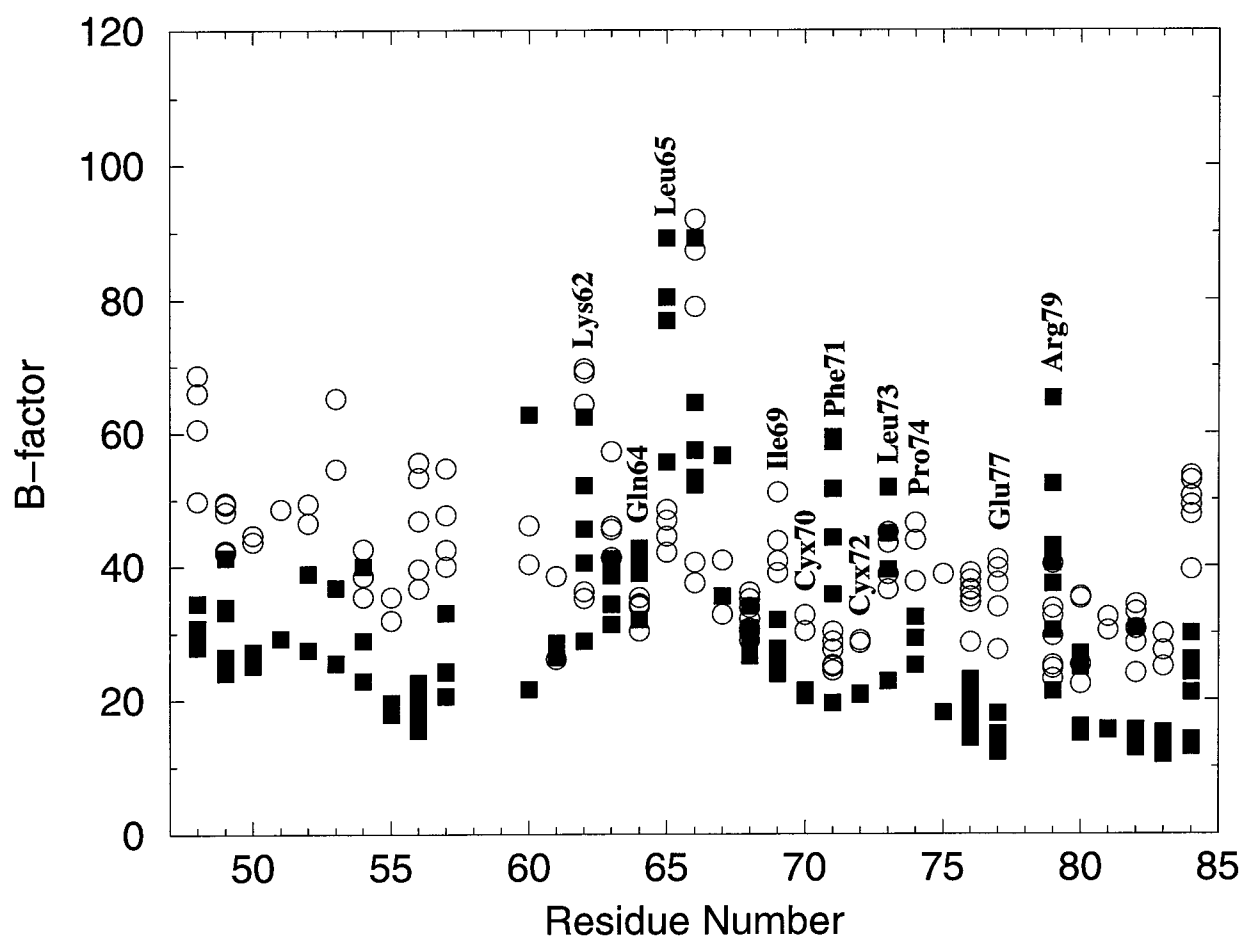
FIGURE 6 Experimental (for x-ray crystal factor VIIa/TF: ○) and calculated (for TF-unbound factor VIIa in solution: ■) B-factors of side-chain heavy atoms of the residues (48–84) in the EGF1 domain. Residues bound to (or in the vicinity of) TF in the TF-bound crystal configuration of factor VIIa are labeled.

the EGF2 domain make direct TF contacts, and apparently all are in the segment 85–93. Neither TF residues nor SP domain residues make crystal contacts with the residues in the segment 103–111. Retention of the overall fold of this domain is not surprising, because it has been shown that the epidermal growth factor-like domains of factor VIIa remain stable under high guanidine hydrochloride concentrations and at elevated temperatures (Freskgard et al., 1998).

Calcium binding to the EGF1 domain

The calcium binding site in EGF1 extends from the N-terminus residues of the EGF1 domain to residues interior to the EGF1 domain. It has been suggested that the calcium binding to the EGF1 domain has no direct effect on contacts with TF residues (Persson and Petersen, 1995), but that the overall docking is enhanced through a Gla-EGF1 orientation stabilized by calcium binding. Kelly et al. (1997) observed significant reduction of TF binding due to Gly, Ala, and Glu replacements of Asp[46]. The loss of function was argued to be due to increased flexibility of the Gla domain relative to the EGF1 domain. Structure analysis of the

relative orientation of Gla and EGF1 domains in factor X, using combined NMR-small angle x-ray scattering techniques, has shown that the relative orientations of the Gla and EGF1 domains depend on calcium binding to the latter domain (Sunnerhagen et al., 1995). In Fig. 8 *a*, we display the Gla/EGF1 domains and the calcium ion present near the junction of these two domains. The calcium ion in the x-ray crystal structure of factor VIIa/TF was found to be octahedrally coordinated with six oxygen ligands from Asp[46]: OD2, Gly[47]:O, GLN[49]:OE1, Asp[63]:OD1 and OD2, and Gln[64]:O. In this "pseudo-octahedral" configuration, four corners are occupied by oxygen atoms, and the fifth corner by the Asp[63] carboxylate. The sixth corner was assumed to be occupied by a water molecule. Nuclear magnetic resonance experiments (Sunnerhagen et al., 1995) revealed that the analogous residues in the EGF1 domain of factor X were in contact with the calcium ion. No contacts in the TF-free solution simulation structure were lost compared to the TF-bound x-ray crystal configuration (see Fig. 8 *b*), and in fact, two additional water molecules were accommodated in its coordination sphere in the TF-free solution structure. These water molecules remained rather immobile during the
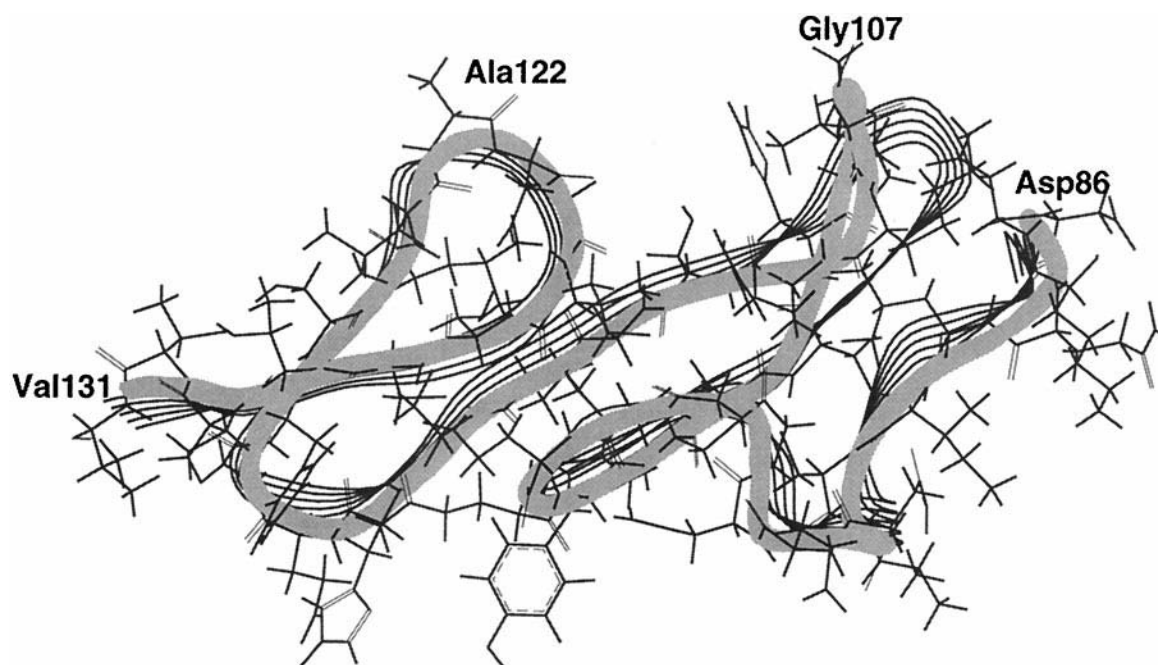
FIGURE 7   Comparison of the final TF-free solution structure (600 ps) of the EGF2 domain of factor VIIa (*light band*) with that of the factor VIIa/TF x-ray crystal complex (*line ribbons*). The least-squares fit of the backbone atom positions was used for the alignment. Side chains are displayed for the solution structure.

trajectory calculation; however, one of the carboxylate oxygen atoms of Asp^{63} moves in and out of the coordination shell of the EGF1-bound calcium ion. In fact, the solution coordination shell of calcium can be recognized as a "pseudopentagonal bipyramid," especially in the situation where only one Asp^{63} oxygen participates in the coordination of calcium (see Fig. 8 *c*). In this structure, calcium is surrounded by a pentagon composed of Gly^{47}:O, Gln^{49}:OE1, Gln^{64}:O, and the oxygen centers from the two water molecules at the vertices. Asp^{46}:OD2 and Asp^{63}:OD1 can be found as apical ligands. When both carboxylic oxygens are in the coordination shell, the structure is still "pseudopentagonal bipyramidal," with Asp^{63} as a double ligand at an apical site (see Fig. 8 *d*).

The electrostatic potential surface around the calcium ion bound to the EGF1 domain is highly electronegative (*circled* in Fig. 9 *a*). The figure was created (GRASP; Nicholls et al., 1993) after removal of the calcium ion from the equilibrated solution structure for which calcium was present in the dynamical steps. This region is approximately neutral (in charge) with the calcium ion in place (Fig. 9 *b*).

The calcium ion from the EGF1 domain was removed in the latter part of our simulation (after 600 ps) to assess its structural importance. The response of the system due to removal of the calcium ion bound to the EGF1 domain can be viewed directly from the changes observed in the RMSDs after 600 ps (Fig. 2). No observable changes appear to be associated with the individual Gla and EGF2 domains due to removal of this calcium ion. A significant increase in the RMSD (from 0.5 to 1.5 Å) of EGF1 is observed in the latter part of the trajectory, indicating some restructuring in

the EGF1 domain. The RMSDs for the EGF1 domain shown in Fig. 2 were calculated by using residues 46–84. To obtain further information about why the total RMSD is larger than before removal of the calcium ion and which residues contribute to the enlarged RMSD, we have examined the RMSDs of the individual residues in the EGF1 domain. The reference system was the crystal configuration. These RMSDs averaged over 25 ps (the segment between 570 and 600 ps for the system with calcium bound to the EGF1 domain and the segment between 1420 and 1445 ps after removal of that calcium) were displayed against the residue numbers in Fig. 10. The content of the figure was made similar to figure 5 of Muranyi et al. (1998) to facilitate the direct comparison of simulation and experiment, and hence the alignment was done using residues 49–84. Note that this selection is different from the original selection of residues 46–83 used in the calculation of total RMSD of the EGF1 domain in Fig. 2. In the work of Muranyi et al. (1998), the solution structure of a synthetic N-terminal EGF-like domain from human factor VII was determined in the absence of calcium ions, using ^{1}H NMR spectroscopy. Comparison of the simulation and experiment (figures 9 and 5 of Muranyi et al., 1998) shows that the simulation captures all features of major structural rearrangement due to the loss of calcium observed in experiment. The EGF1 domain structure is changed only in the regions for which the calcium ion had contacts, and the changes are found to be significant only for a few residues at the N-terminus of the EGF1 domain. Comparison of the calcium bound structure (*dotted line*) to the calcium removed structure (*solid line*) results in the observation that residues around Gln^{64}
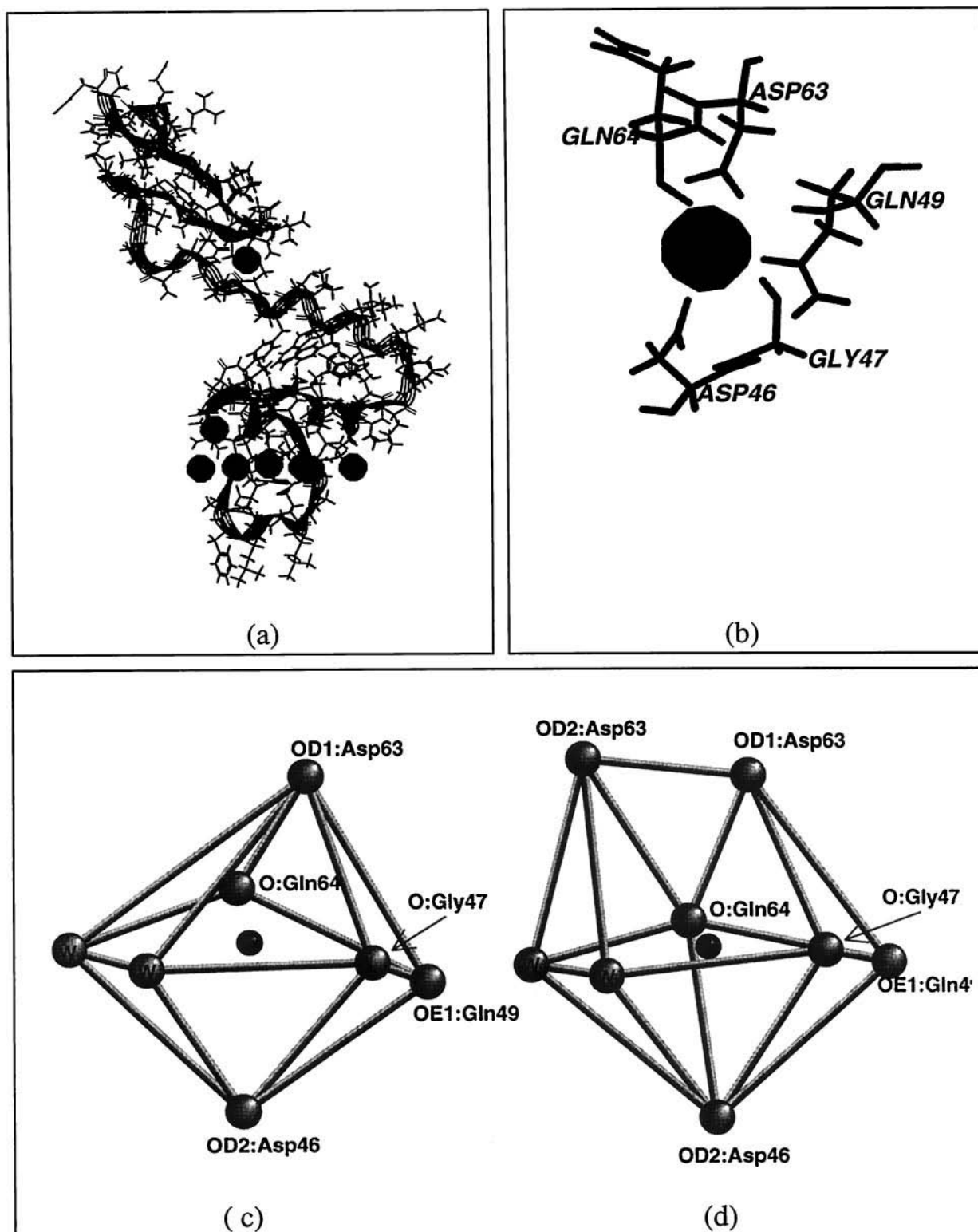
FIGURE 8 (*a*) The final TF-free solution structure (600 ps) of the Gla/EGF1 domains of factor VIIa. All of the calcium ions in the Gla and EGF1 regions are displayed along with the hydrophobic residues (Phe[4], Leu[5], and Leu[8]) in the Gla domain that are thought to interact with phospholipid upon lipid binding. (*b*) The residues in the EGF1 domain solution structure that coordinate with the calcium ion. The coordinated water molecules are not shown. (*c*) The solution "pseudo-pentagonal pyramidal" structure of the calcium ion coordinated to the EGF1 domain. Oxygens of the two water molecules (*dark circles and unmarked*), along with O:Gln[64], OE1:Gln[49] and O:Gly[47], form the pentagon, and OD1:Asp[63] and OD2:Asp[46] are located at the apical positions. The calcium ion is at the center. (*d*) A frequently populated coordinate shell during the simulation. In addition to the atoms found in *c*, OD2:Asp[63] also participates in the coordination of calcium.
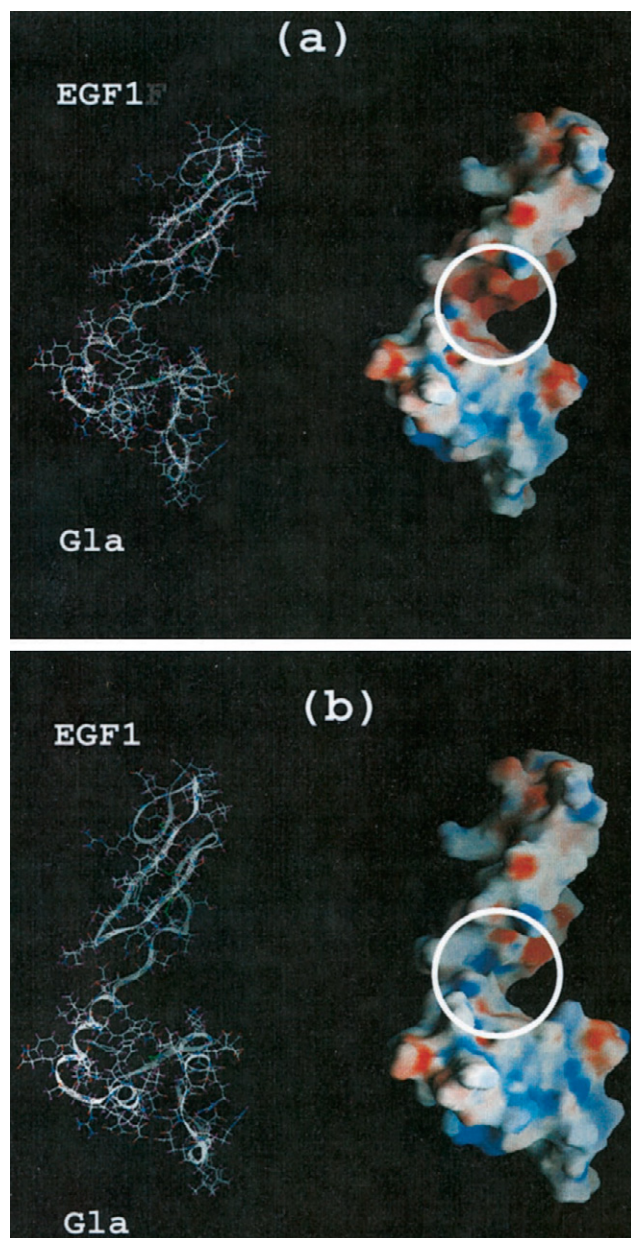
FIGURE 9　Electrostatic potential surfaces calculated for residues 1–84 in the TF-free solution structure. The program GRASP (Nicholls et al., 1993) was used to construct the surface. All calcium ions except the one bound to the EGF1 domain are present in the surface construction. (*a*) The calcium ion was removed (600 ps). The dark red patch in the middle (*circled*) represents the electronegative region to which the calcium ion is bound. (*b*) With the calcium in place, the electrostatic potential (in the *circled region*) shows neutrality.
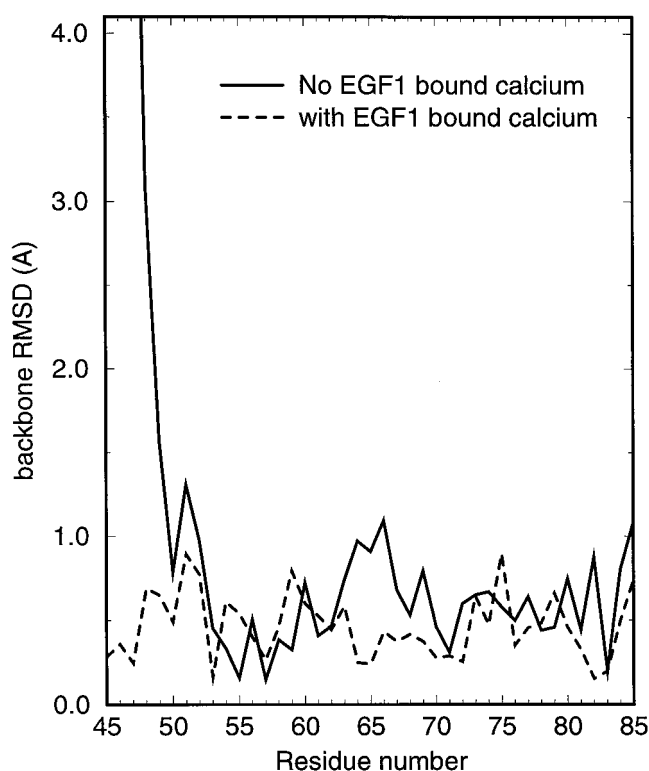

FIGURE 10　Backbone atom displacements of the EGF1 residues. The deviations were calculated with respect to the crystallographic positions. Calcium free (———) and EGF1 bound calcium (– – –). In the calculation of backbone RMSDs, the systems are aligned with residues 49–84 to facilitate comparison with experiment (Muranyi et al., 1998).

have slightly perturbed backbone positions. Interestingly, a majority of the residues in this domain help maintain secondary structure when the calcium ion is removed. This observation is emphasized from the backbone C_α superimposition shown in Fig. 11 for the TF-bound crystal and the two TF-free solution structures.

Before removal of the calcium bound to the EGF1 domain, the observed RMSDs for the combined Gla/EGF1 domains and EGF1/EGF2 domains are somewhat larger than RMSDs for the individual domains (see Fig. 2). The larger RMSDs suggest possible interdomain motions, especially in the case of Gla/EGF1, because the individual domains display much smaller RMSDs. A reasonable check for the possibility of interdomain motion can be obtained by viewing the snapshots of the backbone structure after aligning them. In Fig. 12, we display the backbone ribbon structures for the TF-bound crystal (*dark band*) and the TF-free solution before (*lighter band* in Fig. 12 *a*) and after (*lighter band* in Fig. 12 *b*) the removal of calcium bound to the EGF1 domain. Because the EGF1 domain is common for both the Gla/EGF1 and EGF1/EGF2 combined domains, the EGF1 domain (residues 46–84) is used for the alignment. Although there is not a perfect match of each domain, the factor VIIa domains in solution are spatially close to those in the factor VIIa/TF crystal. This spatial correspondence of the three domains leads to the conclusion that there is no significant alteration in the length of the light chain of factor VIIa along the long axis through interdomain movement due to the association with TF. This is in good agreement with the experimental finding (using x-ray and neutron scattering on the factor VIIa in TF-free and TF-bound forms in solution) that in solution, factor VIIa has an extended or elongated domain structure, providing a large surface area for interaction with TF to form a high-affinity complex (Ashton et al., 1998). It is interesting that the RMSDs of TF
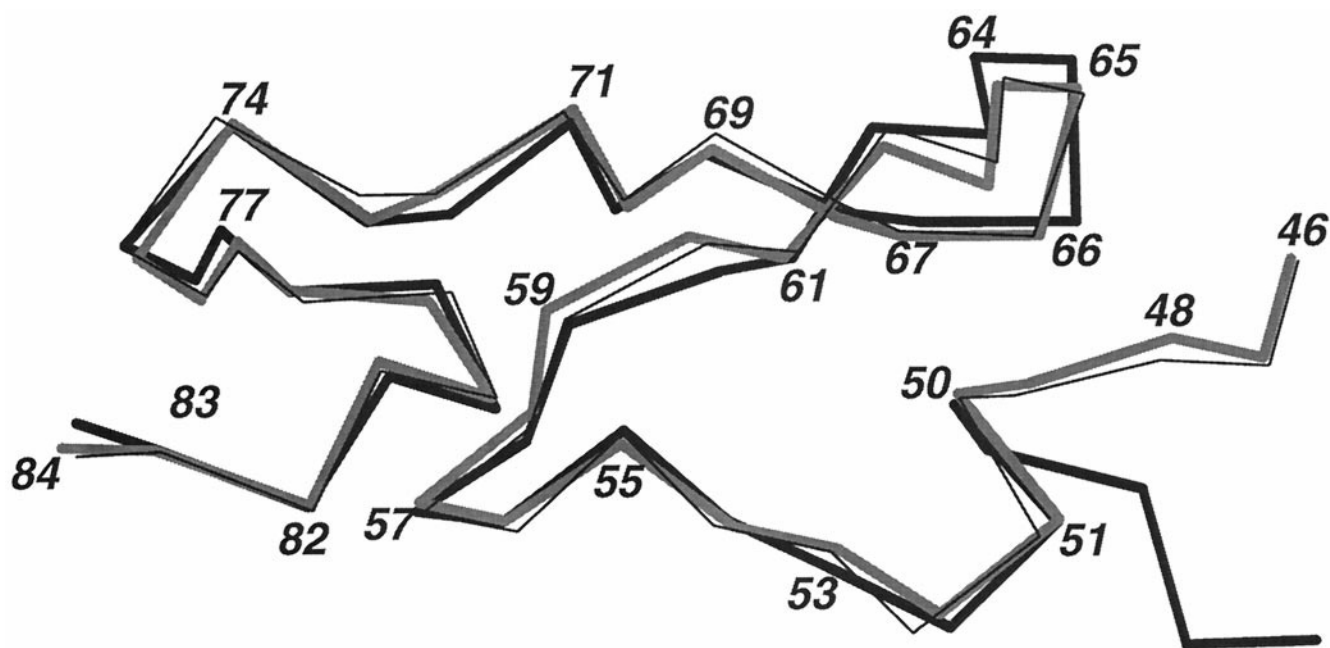
FIGURE 11   Alignment of the C$_\alpha$ positions of the EGF1 domains for the TF-bound crystal (*thin dark line in both panels*), TF-free solution (*thick lighter line*), TF-free solution without calcium (*thick dark line*). The TF-free solution structures were aligned with residues 49–84 of the TF-bound crystal structure.

coordinates in crystal (Harlos et al., 1994; pdb entry = 1boy), when aligned with TF coordinates in the factor VIIa/TF complex (pdb entry = 1dan), are 1.37 Å (heavy atoms) and 0.86 Å (backbone atoms). Thus we might predict minimal restructuring of the components of the factor VIIa/TF complex during the protein-protein complexation. However, once aligned using the EGF1 domain residues, the positions of the backbone atoms of the Gla domain residues in solution are shifted by ~3–4 Å, on average, from the crystal positions toward the space occupied by TF. Still, the orientation of the Gla domain in solution remains rather parallel to that of the TF-bound crystal form. Meanwhile, the backbone atoms of the residues in the EGF2 domain in solution (once the EGF1 residues are aligned) move 5–6 Å, on average, away from the crystal positions.

On the other hand, removal of the calcium brings much larger changes to the Gla EGF1 orientation (Fig. 12 *b*). Both RMSD (Fig. 2) and the backbone ribbon diagram (Fig. 12 *b*) convincingly illustrate such large deviations. In the pictured alignment, the backbone atoms of the Gla domain residues in solution show 15–20-Å deviations from the crystal positions. However, the deviations in the backbone atoms of the EGF2 domain residues are rather comparable with those found in solution with the EGF1-bound calcium intact. Even after the removal of the EGF1-bound calcium ion, spatial arrangement of the three domains predicts that the light chain of factor VIIa shows only ~2–3% reduction in its chain length compared to that of TF-bound crystal.

The Gla domain is thought to be responsible for lipid binding (Pollock et al., 1988; Wildgoose et al., 1992). The interaction of the Gla domain with the lipid surface has been proposed to be via calcium bridging (Nelsestuen, 1988) or

through insertion of hydrophobic residues to the lipid surface (Ellison and Castellino, 1997). Although there is a slight Gla-EGF1 reorientation in solution with TF absent, the spatial arrangement that may be provided for lipid binding appears similar in TF-free solution and TF-bound crystal structures. A major spatial realignment of the Gla and EGF1 domains would be required in the case for which the EGF1-bound calcium is absent, to bring the two domains into an orientation suitable for both TF and lipid binding. Fig. 12 emphasizes that the calcium ion bound to the EGF1 domain is critical for bringing the two domains (Gla and EGF1) into the correct orientation for factor VII's TF binding in solution.

We do not find direct domain-domain interactions via H-bonding or salt bridges in the predicted TF-free solution structure or in the TF-bound x-ray crystal structure. However, the two neighboring domains are connected via a segment of amino acid residues. For the Gla and EGF1 domains, the segment of residues 36–45 acts as the connecting region, whereas for the EGF1 and EGF2 domains residues 84–86 provide this function. The amino acid residues found in the connecting region can make H-bonds individually with domains that they connect. Depending on the length of the connecting region, this situation can confer a flexibility on the domain alignments.

In the present work we have assessed the importance of the calcium ion bound to the EGF1 domain in TF binding. Furthermore, comparison of the TF-free solution structure with the TF-bound crystal was used to understand how the EGF1 domain responds to TF binding. A complete picture of the response of factor VIIa to the interaction with TF may
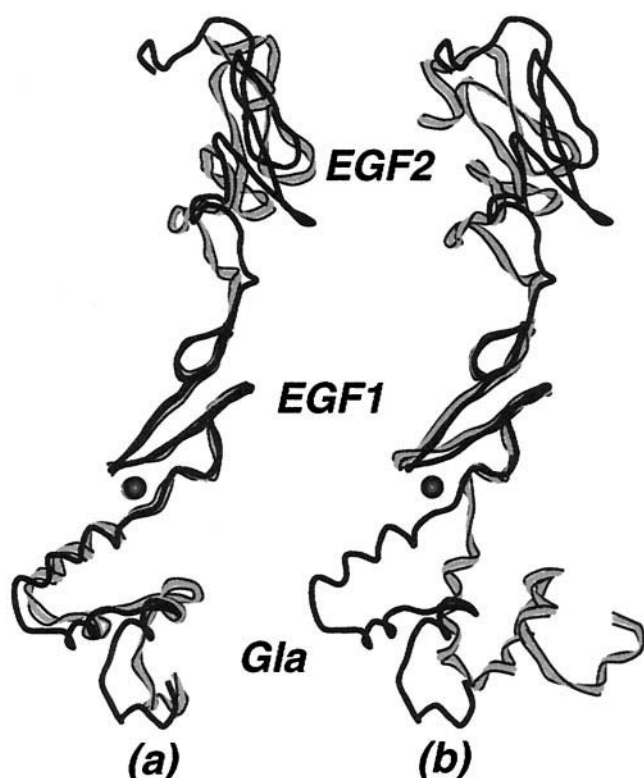
FIGURE 12   Backbone alignment of the light chain of factor VIIa in the TF-bound crystal (*dark line*) and in TF-free solution (*light line*). (*a*) The EGF1 bound calcium ion is present (solution structure, 600 ps). (*b*) After removal of EGF1 bound calcium (solution structure, 845 ps after the calcium is removed). Residues 1–131 (Gla, EGF1, and EGF2) of the x-ray crystal structure were used for the alignment. Because the importance of the presence of the calcium bound to the EGF1 domain is emphasized, that calcium is also included in the figure (*sphere in the middle*). The dark and light spheres in *a* correspond to the calcium ion in crystal and in solution, respectively (indistinguishable because of close encounter). Panel *b* contains only the calcium ion in the x-ray crystal structure.

be obtained by including all domains of factor VIIa in the simulation; this is currently under way in our laboratory.

CONCLUSIONS

We have used molecular dynamics simulations to estimate the solution structure of the light chain of factor VIIa in the absence of TF. The domain structures (Gla, EGF1, and EGF2) are found to be very similar to the corresponding domains of the factor VIIa/TF complex of the x-ray crystal form. No significant change in the chain length along the long axis of factor VIIa compared to its activated, tissue factor-bound form is observed during the 600-ps simulation. This is in good agreement with experimental findings (Ashton et al., 1998), for which the solution domain structure of factor VIIa appears extended. However, we find relative domain-domain movements for both Gla/EGF1 and EGF1/EGF2 domains. Furthermore, no direct interdomain salt bridges or H-bonds are found in the TF-free solution structure.

The Ala[1] network (in the formation of Ω-loop) and the calcium-Gla network found in the x-ray crystal configuration of TF-bound factor VIIa are preserved in the solution structure of TF-free factor VIIa. The features of the Gla domain solution structure of factor VIIa are very similar to those found in the solution structure of the Gla domain of BF1. It appears reasonable that the Ala[1] network in BF1 is responsible for the phospholipid binding conformation of the Ω-loop (residues 1–11), with the calcium-Gla network providing the correct folding for lipid binding. Similarities observed in the above networks of factor VIIa and BF1 indicate similar mechanisms for lipid binding.

The coordination of the calcium ion to protein atoms present near the connecting region of the Gla and EGF1 domains to the amino acid residues in these domains remains unchanged in the solution structure without TF, whereas the coordination shell that is partially saturated in the x-ray crystal structure (six bonds) extends its coordination number to 8 by including two water molecules in the coordination shell in the solution structure. We find that removal of this calcium ion leads to only minor structural changes in the EGF1 domain of the TF-free solution structure, but the Gla-EGF1 relative orientation is substantially disturbed. Our simulation results agree well with the experimental finding of minimal structural changes in the EGF1 domain associated with the calcium binding to that domain (Muranyi et al., 1998). Furthermore, the current simulation provides a prediction for an altered relative orientation between the Gla and EGF1 domains resulting from calcium binding, similar to the finding of Gla-EGF1 reorientation for factor X from combined NMR–small-angle x-ray scattering experiments (Sunnerhagen et al., 1995).

REFERENCES

Ashton, A. W., M. K. Boehm, D. J. Johnson, G. Kemball-Cook, and S. J. Perkins. 1998. The solution structure of human coagulation factor VIIa in its complex with tissue factor is similar to free factor VIIa: a study of a heterodimeric receptor-ligand complex by x-ray and neutron scattering and computational modeling. *Biochemistry.* 37:8208–8217.

Banner, D. W. 1997. The factor VIIa/tissue factor complex. *Thromb. Haemost.* 78:512–515.

Banner, D. W., A. D'Arcy, C. Chene, F. Vilbois, W. H. Konigsberg, A. Guha, Y. Nemerson, and D. Kirchhofer. 1995. The crystal structure of the complex of human factor VIIa with human soluble tissue factor. *Thromb. Haemost.* 73:1183–1183.

Banner, D. W., A. D'Arcy, C. Chene, F. K. Winkler, A. Guha, W. H. Konigsberg, Y. Nemerson, and D. Kirchhofer. 1996. The crystal structure of the complex of blood coagulation factor VIIa with soluble tissue factor. *Nature.* 380:41–46.

Berube, C., F. A. Ofosu, J. G. Kelton, and M. A. Blajchman. 1992. A novel congenital haemostatic defect: combined factor VII and factor XI deficiency. *Blood Coagul. Fibrinolysis.* 3:357–360.

Bjoern, S., D. C. Foster, L. Thim, F. C. Wiberg, M. Christensen, Y. Komiyama, A. H. Pedersen, and W. Kisiel. 1991. Human plasma and recombinant factor VII—characterization of *O*-glycosylations at serine residues-52 and residues-60 and effects of site-directed mutagenesis of serine-52 to alanine. *J. Biol. Chem.* 266:11051–11057.

Butenas, S., and K. G. Mann. 1996. Kinetics of human factor VII activation. *Biochemistry.* 35:1904–1910.

Chaing, S., B. Clarke, S. Sridhara, K. Chu, P. Friedman, W. VanDusen, H. R. Roberts, M. Blajchman, D. M. Monroe, and K. A. High. 1994. Severe factor VII deficiency caused by mutations abolishing the cleavage site for activation and altering binding to tissue factor. *Blood.* 83:3524–3535.

Cheung, W. F., and D. W. Stafford. 1995. Localization of an epitope of a calcium-dependent monoclonal antibody to the N-terminal region of the Gla domain of human factor VII. *Thromb. Res.* 79:199–206.

Cooper, D. N., D. S. Millar, A. Wacey, D. W. Banner, and E. G. Tuddenham. 1997. Inherited factor VII deficiency: molecular genetics and pathophysiology. *Thromb. Haemost.* 78:151–160.

Cornell, W. D., P. Cieplak, C. I. Bayly, I. R. Gould, K. M. Merz, Jr., D. M. Ferguson, D. C. Spellmeyer, T. Fox, J. W. Caldwell, and P. A. Kollman. 1995. A new force field for molecular mechanical simulation of nucleic acids and proteins. *J. Am. Chem. Soc.* 117:5179–5197.

Davie, E. W. 1995. Biochemical and molecular aspects of the coagulation cascade. *Thromb. Haemost.* 74:1–6.

Dickinson, C. D., C. R. Kelly, and W. Ruf. 1996. Identification of surface residues mediating tissue factor binding and catalytic function of the serine protease factor VIIa. *Proc. Natl. Acad. Sci. USA.* 93: 14379–14384.

Dickinson, C. D., and W. Ruf. 1997. Active site modification of factor VIIa affects interactions of the protease domain with tissue factor. *J. Biol. Chem.* 272:19875–19879.

Edgington, T. S., C. D. Dickinson, and W. Ruf. 1997. The structural basis of function of the TF. VIIa complex in the cellular initiation of coagulation. *Thromb. Haemost.* 78:401–405.

Ellison, E. H., and F. J. Castellino. 1997. Adsorption of bovine prothrombin to spread phospholipid monolayers. *Biophys. J.* 72:2605–2615.

Essmann, U., L. Perera, M. L. Berkowitz, T. Darden, H. Lee, and L. G. Pedersen. 1995. A smooth particle mesh Ewald method. *J. Chem. Phys.* 103:8577–8593.

Freskgard, P. O., L. C. Petersen, D. A. Gabriel, X. Li, and E. Persson. 1998. Conformational stability of factor VIIa: biophysical studies of thermal and guanidine hydrochloride-induced denaturation. *Biochemistry.* 37: 7203–7212.

Geng, J. P., and F. J. Castellino. 1997. Properties of a recombinant chimeric protein in which the gamma-carboxyglutamic acid and helical stack domains of human anticoagulant protein C are replaced by those of human coagulation factor VII. *Thromb. Haemost.* 77:926–933.

Hagen, F. S., C. L. Gray, P. O'Hara, F. J. Grant, G. C. Saari, R. G. Woodbury, C. E. Hart, M. Insley, W. Kisiel, and K. Kurachi. 1986. Characterization of a cDNA coding for human factor VII. *Proc. Natl. Acad. Sci. USA.* 83:2412–2416.

Hamaguchi, N., P. Charifson, T. Darden, L. Xiao, K. Padmanabhan, A. Tulinsky, R. Hiskey, and L. Pedersen. 1992. Molecular dynamics simulation of bovine prothrombin fragment 1 in the presence of calcium ions. *Biochemistry.* 31:8840–8848.

Harlos, K., D. M. Martin, D. P. O'Brien, E. Y. Jones, D. I. Stuart, I. Polikarpov, A. Miller, E. G. Tuddenham, and C. W. Boys. 1994. Crystal structure of the extracellular region of human tissue factor. *Nature.* 370:662–666 (erratum: *Nature.* 1994. 371:720).

Harris, R. J., C. K. Leonard, A. W. Guzzetta, and M. W. Spellman. 1991. Tissue plasminogen activator has an O-linked fucose attached to threonine-61 in the epidermal growth factor domain. *Biochemistry.* 30: 2311–2314.

Harvey, S. C., R. K. Z. Tan, and T. E. Cheatham, III. 1998. The flying ice cube: velocity rescaling in molecular dynamics leads to violation of energy equipartition. *J. Comp. Chem.* 18:726–740.

Iino, M., D. C. Foster, and W. Kisiel. 1998. Functional consequences of mutations in Ser-52 and Ser-60 in human blood coagulation factor VII. *Arch. Biochem. Biophys.* 352:182–192.

Inoue, K., H. Shimada, J. Ueba, S. Enomoto, Y. Tanaka-Saisaka, T. Kubota, M. Koyama, and T. Morita. 1996. High-affinity calcium-binding site in the gamma-carboxyglutamic acid domain of bovine factor VII. *Biochemistry.* 35:13826–13832.

Jesty, J., and S. A. Morrison. 1983. The activation of factor IX by tissue factor-factor VII in a bovine plasma system lacking factor X. *Thromb. Res.* 32:171–181.

Kelly, C. R., C. D. Dickinson, and W. Ruf. 1997. Ca^{2+} binding to the first epidermal growth factor module of coagulation factor VIIa is important for cofactor interaction and proteolytic function. *J. Biol. Chem.* 272: 17467–17472.

Kirchhofer, D., A. Guha, Y. Nemerson, W. H. Konigsberg, F. Vilbois, C. Chene, D. W. Banner, and A. D'Arcy. 1995. Activation of flood coagulation-factor VIIa with cleaved tissue factor extracellular domain and crystallization of the active complex. *Proteins.* 22:419–425.

Kirchhofer, D., and Y. Nemerson. 1996. Initiation of blood coagulation: the tissue factor factor VIIa complex. *Curr. Opin. Biotechnol.* 7:386–391.

Krishnaswamy, S. 1992. The interaction of human factor VIIa with tissue factor. *J. Biol. Chem.* 267:23696–23706.

Laskowski, R. A., M. W. MacArthur, D. S. Moss, and J. M. Thornton. 1993. PROCHECK—a program to check the stereochemical quality of protein structures. *J. Appl. Crysallogr.* 26:283–291.

Lawson, J. H., S. Butenas, and K. G. Mann. 1992. The evaluation of complex-dependent alterations in human factor VIIa. *J. Biol. Chem.* 267:4834–4843.

Lawson, J. H., and K. G. Mann. 1991. Cooperative activation of human factor IX by the human extrinsic pathway of blood coagulation. *J. Biol. Chem.* 266:11317–11327.

Leonard, B. N., Q. Chen, M. A. Blajchman, F. A. Ofosu, S. Sridhara, D. Yang, and B. J. Clarke. 1998. Factor VII deficiency caused by a structural variant N57D of the first epidermal growth factor domain. *Blood.* 91:142–148.

Li, L., T. Darden, C. Foley, R. Hiskey, and L. Pedersen. 1995. Homology modeling and molecular dynamics simulation of human prothrombin fragment 1. *Protein Sci.* 4:2341–2348.

Li, L., T. A. Darden, S. J. Freedman, B. C. Furie, B. Furie, J. D. Baleja, H. Smith, R. G. Hiskey, and L. G. Pedersen. 1997. Refinement of the NMR solution structure of the gamma-carboxyglutamic acid domain of coagulation factor IX using molecular dynamics simulation with initial Ca^{2+} positions determined by a genetic algorithm. *Biochemistry.* 36: 2132–2138.

Li, L., T. Darden, R. Hiskey, and L. G. Pedersen. 1996. Computational studies of human prothrombin fragment 1, the Gla domain of factor IX and several biological interesting mutants. *Haemostasis.* 26(Suppl. 1): 54-9–54-59.

Martin, D. M., D. P. O'Brien, E. G. Tuddenham, and P. G. Byfield. 1993. Synthesis and characterization of wild-type and variant gamma-carboxyglutamic acid-containing domains of factor VII. *Biochemistry.* 32:13949–13955.

McDonald, J. F., T. C. J. Evans, D. B. Emeagwali, M. Hariharan, N. M. Allewell, M. L. Pusey, A. M. Shah, and G. L. Nelsestuen. 1997a. Ionic properties of membrane association by vitamin K-dependent proteins: the case for univalency. *Biochemistry.* 36:15589–15598.

McDonald, J. F., A. M. Shah, R. A. Schwalbe, W. Kisiel, B. Dahlback, and G. L. Nelsestuen. 1997b. Comparison of naturally occurring vitamin K-dependent proteins: correlation of amino acid sequences and membrane binding properties suggests a membrane contact site. *Biochemistry.* 36:5120–5127.

Meade, T. W. 1983. Factor VII and ischaemic heart disease: epidemiological evidence. *Haemostasis.* 13:178–185.

Muranyi, A., B. E. Finn, G. P. Gippert, S. Forsen, J. Stenflo, and T. Drakenberg. 1998. Solution structure of the N-terminal EGF-like domain from human factor VII. *Biochemistry.* 37:10605–10615.

Nakagaki, T., P. Lin, and W. Kisiel. 1992. Activation of human factor VII by the prothrombin activator from the venom of *Oxyuranus scutellatus* (Taipan snake). *Thromb. Res.* 65:105–116.

Nelsestuen, G. L. 1988. Basis for prothrombin-membrane binding. *In* Current Advances in Vitamin K Research. J. W. Suttie, editor. Elsevier Science Publishing, New York.

Nemerson, Y. 1988. Tissue factor and hemostasis. *Blood.* 71:1–8 (erratum: *Blood.* 1988. 71:1178).

Nemerson, Y., and M. P. Esnouf. 1973. Activation of a proteolytic system by a membrane lipoprotein: mechanism of action of tissue factor. *Proc. Natl. Acad. Sci. USA.* 70:310–314.

Nicholls, A., R. Bharadwaj, and B. Honig. 1993. Grasp—graphical representation and analysis of surface properties. *Biophys. J.* 64:A166–A166.

Nishimura, H., S. Kawabata, W. Kisiel, S. Hase, T. Ikenaka, T. Takao, Y. Shimonishi, and S. Iwanaga. 1989. Identification of a disaccharide (xyl-glc) and a trisaccharide (xyl2-glc) O-glycosidically linked to a serine residue in the 1st epidermal growth factor-like domain of human factor-VII and factor-IX and protein-Z and bovine protein-Z. *J. Biol. Chem.* 264:20320–20325.

O'Brien, D. P., G. Kemballcook, A. M. Hutchinson, D. A. Martin, D. D. Johnson, P. H. Byfield, O. Takamiya, E. D. Tuddenham, and J. H. McVey. 1994. Surface-plasmon resonance studies of the interaction between factor-VII and tissue factor—demonstration of defective tissue factor-binding in a variant FVII molecule (FVII-R79Q). *Biochemistry.* 33:14162–14169.

Pearlman, D. A., D. A. Case, J. W. Caldwell, W. S. Ross, T. E. Cheatham, III, D. M. Ferguson, G. L. Seibel, U. C. Singh, P. A. Weiner, and P. A. Kollman. 1995. AMBER4.1. University of California, San Francisco.

Perera, L., T. Darden, and L. G. Pedersen. 1998. *Trans-cis* isomerization of Pro22 in bovine prothrombin fragment 1: a surprising result of structural characterization. *Biochemistry.* 37:10920–10927.

Perera, L., L. Li, T. Darden, D. M. Monroe, and L. G. Pedersen. 1997. Prediction of solution structures of the Ca^{2+}-bound gamma-carboxyglutamic acid domains of protein S and homolog growth arrest specific protein 6: use of the particle mesh Ewald method. *Biophys. J.* 73:1847–1856.

Persson, E. 1996. Influence of the gamma-carboxyglutamic acid-rich domain and hydrophobic stack of factor VIIa on tissue factor binding. *Haemostasis.* 26(Suppl. 1):31-4–31-34.

Persson, E. 1997. Characterization of the interaction between the light chain of factor VIIa and tissue factor. *FEBS Lett.* 413:359–363.

Persson, E., and L. S. Nielsen. 1996. Site-directed mutagenesis but not gamma-carboxylation of Glu-35 in factor VIIa affects the association with tissue factor. *FEBS Lett.* 385:241–243.

Persson, E., O. H. Olsen, A. Ostergaard, and L. S. Nielsen. 1997. Ca^{2+} binding to the first epidermal growth factor-like domain of factor VIIa increases amidolytic activity and tissue factor affinity. *J. Biol. Chem.* 272:19919–19924.

Persson, E., and L. C. Petersen. 1995. Structurally and functionally distinct Ca^{2+} binding sites in the gamma-carboxyglutamic acid-containing domain of factor VIIa. *Eur. J. Biochem.* 234:293–300.

Petersen, L. C., S. Valentin, and U. Hedner. 1995. Regulation of the extrinsic pathway system in health and disease: the role of factor VIIa and tissue factor pathway inhibitor. *Thrombosis Res.* 79:1–47.

Petersen, L. C., and E. Persson. 1996. Effect of Ca^{2+} on the structure and function of factor VIIa. *Haemostasis.* 26(Suppl. 1):40-4–40-44.

Pollock, J. S., A. J. Shepard, D. J. Weber, D. L. Olson, D. G. Klapper, L. G. Pedersen, and R. G. Hiskey. 1988. Phospholipid binding properties of bovine prothrombin peptide residues 1–45. *J. Biol. Chem.* 263: 14216–14223.

Rapaport, S. I., and L. V. Rao. 1995. The tissue factor pathway: how it has become a "prima ballerina." *Thromb. Haemost.* 74:7–17.

Ruf, W. 1994. Factor VIIa residue Arg290 is required for efficient activation of the macromolecular substrate factor X. *Biochemistry.* 33: 11631–11636.

Sakai, T., T. Lund-Hansen, L. Paborsky, A. H. Pedersen, and W. Kisiel. 1989. Binding of human factors VII and VIIa to a human bladder carcinoma cell line (J82). Implications for the initiation of the extrinsic pathway of blood coagulation. *J. Biol. Chem.* 264:9980–9988.

Selander-Sunnerhagen, M., M. Ullner, E. Persson, O. Teleman, J. Stenflo, and T. Drakenberg. 1992. How an epidermal growth factor (EGF)-like domain binds calcium. High resolution NMR structure of the calcium form of the NH2-terminal EGF-like domain in coagulation factor X. *J. Biol. Chem.* 267:19642–19649.

Sunnerhagen, M., S. Forsen, A. M. Hoffren, T. Drakenberg, O. Teleman, and J. Stenflo. 1995. Structure of a Ca^{2+}-free gla domain sheds light on membrane- binding of blood-coagulation proteins. *Thromb. Haemost.* 73:1207–1207.

Sunnerhagen, M. S., E. Persson, I. Dahlqvist, T. Drakenberg, J. Stenflo, M. Mayhew, M. Robin, P. Handford, J. W. Tilley, and I. D. Campbell. 1993. The effect of aspartate hydroxylation on calcium binding to epidermal growth factor-like modules in coagulation factors IX and X. *J. Biol. Chem.* 268:23339–23344.

Takamiya, O., S. Abe, A. Yoshioka, K. Nakajima, J. H. McVey, and E. G. Tuddenham. 1995. Factor VIIShinjo: a dysfunctional factor VII variant homozygous for the substitution Gln for Arg at position 79. *Haemostasis.* 25:89–97.

Thim, L., S. Bjoern, M. Christensen, E. M. Nicolaisen, T. Lundhansen, A. H. Pedersen, and U. Hedner. 1988. Amino-acid sequence and post-translational modifications of human factor-VIIa from plasma and transfected baby hamster- kidney cells. *Biochemistry.* 27:7785–7793.

Triplett, D. A., J. T. Brandt, M. A. Batard, J. L. Dixon, and D. S. Fair. 1985. Hereditary factor VII deficiency: heterogeneity defined by combined functional and immunochemical analysis. *Blood.* 66:1284–1287.

Tuddenham, E. G. 1996. The tissue factor-factor VII complex: recent advances towards elucidating the structure and function of the initiator of haemostasis. *Haemostasis.* 26(Suppl. 1):20-4–20-24.

Tuddenham, E. G. D., and D. N. Cooper. 1994. The Molecular Genetics of Haemostasis and Its Inherited Disorder. Oxford University Press, New York.

Tuddenham, E. G., S. Pemberton, and D. N. Cooper. 1995. Inherited factor VII deficiency: genetics and molecular pathology. *Thromb. Haemost.* 74:313–321.

Welsch, D. J., and G. L. Nelsestuen. 1988. Amino-terminal alanine functions in a calcium-specific process essential for membrane binding by prothrombin fragment 1. *Biochemistry.* 27:4939–4945.

Wildgoose, P., K. L. Berkner, and W. Kisiel. 1990. Synthesis, purification, and characterization of an Arg152–Glu site-directed mutant of recombinant human blood clotting factor VII. *Biochemistry.* 29:3413–3420.

Wildgoose, P., T. Jorgensen, Y. Komiyama, T. Nakagaki, A. Pedersen, and W. Kisiel. 1992. The role of phospholipids and the factor VII Gla-domain in the interaction of factor VII with tissue factor. *Thromb. Haemost.* 67:679–685.

Yamamoto, M., T. Nakagaki, and W. Kisiel. 1992. Tissue factor-dependent autoactivation of human blood coagulation factor VII. *J. Biol. Chem.* 267:19089–19094.

Zur, M., and Y. Nemerson. 1978. The esterase activity of coagulation factor VII. Evidence for intrinsic activity of the zymogen. *J. Biol. Chem.* 253:2203–2209.